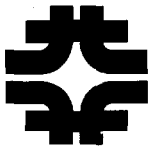

Fermilab

TM-641
1600
1/30/76

SUPERCONDUCTING WIRE STABILITY WORKSHOP/July 22, 1974

Superconducting Group
Fermi National Accelerator Laboratory
P.O. Box 500
Batavia, Illinois 60510

SUPERCONDUCTING WIRE STABILITY WORKSHOP

TOPICS

July 22, 1974

1. Cryogenic Stability
   Instabilities Due to the Bean Model

   Prof. Roger Boom
   University of Wisconsin - Madison

2. The Effects of Non-Linear Heat Transfer
   Terminal Characteristics
   Stability Map

   Bruce Strauss
   Fermilab - Energy Doubler

3. Dynamic Stability

   Darrell Drickey
   Fermilab - Energy Doubler

4. Adiabatic Stability

   Phil Sanger
   Fermilab - Energy Doubler

5. Mechanical Instabilities

   Joe Heim
   Fermilab - Research Services

INTRODUCTION

One of the major problems that has been encountered in designing and building superconducting magnets is the failure of the wire, when wound into a magnet, to perform to its short sample limit. Typically the wire in the magnet will transition from the superconducting to normal state, or "quench", at an operating current and associated field much less than predicted by short sample data. In addition, the magnet will exhibit "training", a phenomena wherein higher and higher limiting currents are attained on each successive quench. Sometimes a magnet will train up to the short sample limit, but in other cases a limiting current is reached that is still much less than short sample.

The problem of training has appeared at one time or another in almost every major superconducting magnet development program, and many explanations for the causes and many remedies have been proposed. Excessive training has been a major concern in the development of a 45 kilogauss Energy Doubler dipole magnet. Stability characteristics of superconducting wire, or more simply the ability of the material to withstand local temperature rises gracefully, are bound up closely with the problem of training, di/dt sensitivity and ac loss characteristics. When a wire is unstable, it will be more prone to generate quenches; there will be a low threshold of quench mode excitation.

In order to acquaint persons associated with the Energy Doubler project with some of the theoretical background material pertaining to stability, and in order to promote a more extensive dialog about some of the performance characteristics of the magnets, a workshop on superconducting wire stability was held at Fermilab on July 22, 1974. The notes presented in this report are from the keynote talks given to cover those topics thought to be most germane to our application problems.

The organizers of the workshop would like to thank the speakers for their efforts in preparing the material, giving the talks, leading the discussions and preparing manuscripts.

CRYOGENIC STABILITY AND INSTABILITIES DUE TO THE BEAN MODEL

Prof. Roger W. Boom, Univ. of Wisconsin, Madison

A. Cryogenic Stability

Consider a section of superconductor as shown in Figure 1.

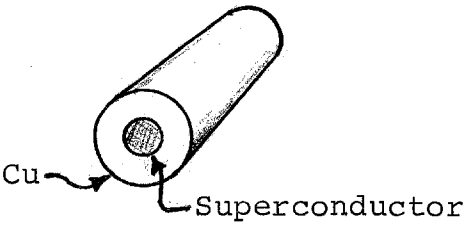

Figure 1.

Considering the superconductor and the copper matrix as a pair of parallel resistors, the sharing of current is described by

$$I_{Tot} = I_{Cu} + I_{SC}$$

and the power dissipated in each branch by

$$P_{SC} = (I_{Tot} - I_{Cu}) I_{Cu} R_{Cu}$$

$$P_{Cu} = I^2_{Cu} R_{Cu}$$

These expressions describe the curves shown in Figure 2. Note that P_{SC} reaches a maximum at $I_{Tot}/2$ and equals one quarter of the maximum value of P_{Cu},

Two other facts are important in determining criteria for cryogenic stability. One is that the short sample curve degrades with increasing temperature, approximately 37%/°K, as shown in Figure 3. The second is the heat transfer characteristic of liquid helium as a function of temperature, shown in Figure 4.

Current in Superconductor, I_{SC} — — — —
Current in copper, I_{Cu} —·—·—
Power in Superconductor, P_{Cu} —··—··—
Power in copper, P_{Cu} ----------

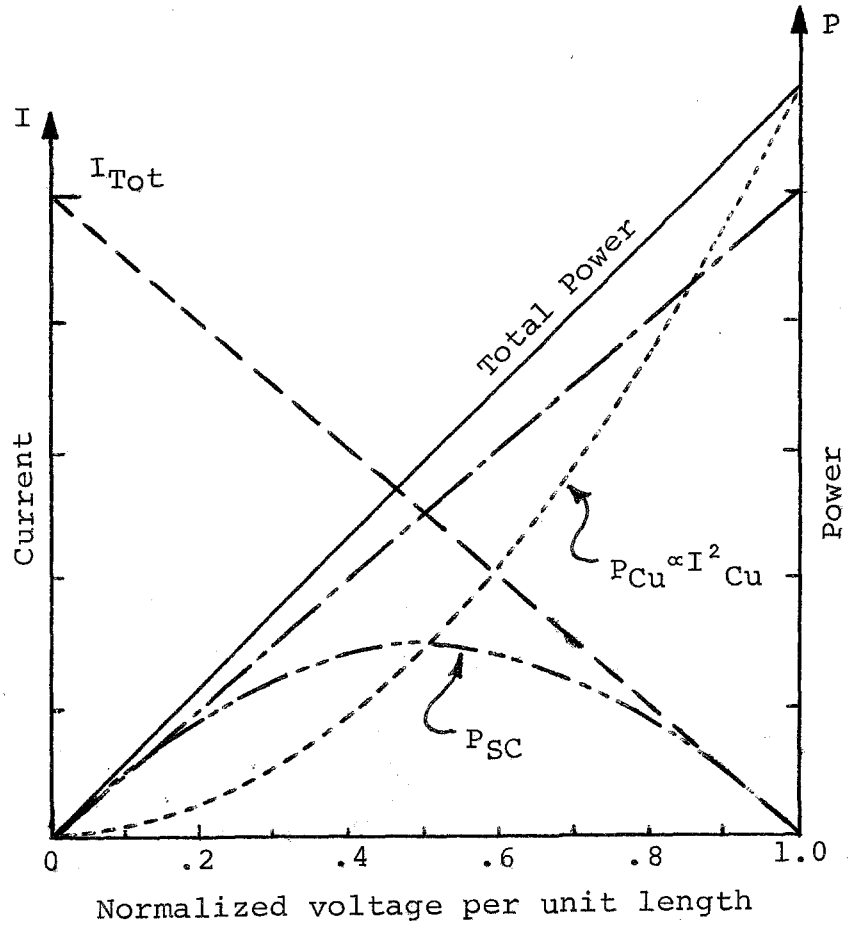

Figure 2. Current sharing and power dissipation characteristics typical of a copper-superconductor matrix.

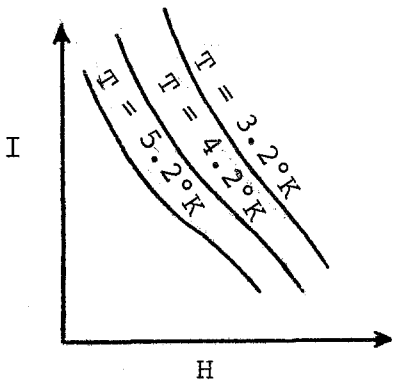

Figure 3.

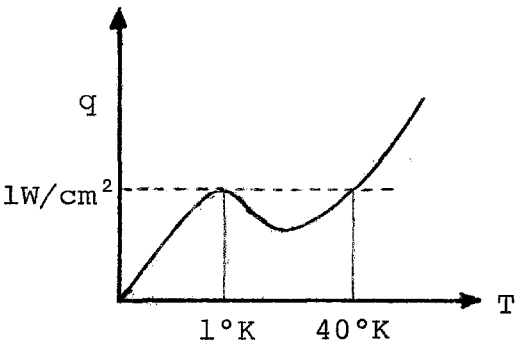

Figure 4.

Now one can set down guidelines for designing a cryogenically stabilized superconductor. The intent is to provide enough low resistivity matrix material and cooling so that: a) all or part of the current can be in the matrix without raising local temperatures to a level that would interfere with normal magnet system operation and b) the conductor will return to the superconducting state when the perturbing heat source is removed. Let us assume that the superconductor is to operate at 4.2 K, then

1. For operation in a liquid helium bath whose temperature is 4.2 K put in enough superconductor to carry all of the current at 5.2 K based on a 37%/ K degradation of the short sample characteristic.
2. With all of the current in the copper matrix one requires

$$I^2_{Tot} R_{Cu} \leq hS\Delta T$$

where h is the heat transfer coefficient to the bath, S the surface area exposed to the helium and ΔT the copper surface to bath temperature difference.

3. Worst case power generation in the superconducting filament occurs with 1/2 of the total current in the superconductor as described above.

Based on items 1 and 3, one calculates the actual temperature of each superconducting filament. In a real wire matrix the temperature distribution will look like that shown in Figure 5.

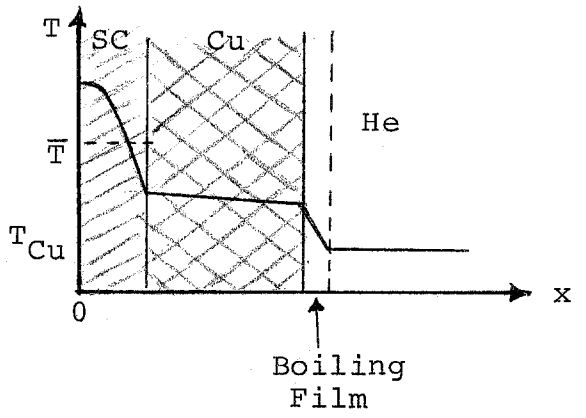

Figure 5.

The temperature drop at the copper-helium interface depends on the maximum heat generated in the composite conductor, $I_{Tot}R_{Cu}$. Typically this ΔT is ~0.25 K at a dissipation of 0.4 watts/cm^2. The Joule heating of the copper matrix also produces a temperature drop across the copper, from the superconducting filament to the helium bath. This ΔT must be calculated for each specific geometry but usually will be

found to be ~0.2 K. Generally, the temperature difference of the superconductor to copper interface is small and in more detailed computations may be accounted for by the addition of a small correction term in the equations for heat generated per unit length.

The maximum temperature rise in a superconducting filament due to maximum Joule heating in that filament can be computed from

$$W_{max} = 8\pi k \ (\overline{T}-T_{Cu})$$

where k is the thermal conductivity of the filament, $\overline{T}$ is the average filament temperature (cf. Figure 5) and T_{Cu} is the copper matrix temperature at the interface with the superconductor. To compute the heat generated per filament

$$W_{max} = \frac{1}{4} \ I^2_{Tot} R_{Cu}$$

must be divided by the number of filaments N. Now the average temperature can be specified, taking into account previously calculated temperature drops. For a 4.2 K bath, a typical value of $\overline{T}$ would be 5.2 K. This information plus the previous two equations allow N to be determined, and then the appropriate filament diameter can be calculated from

$$I_{Tot} = N \ J(T) \pi \frac{d^2}{4}$$

Of the various stabilizing schemes proposed, it generally turns out all one ever really achieves is cryogenic stability.

B. Instabilities Determined from the Bean Model*

Consider a slab of superconducting material as in Figure 6 where the flux penetration is shown for an external field. The general definition of magnetization $\vec{M}$ for a material can be written as

$$\vec{H}-\vec{B} = -4\pi\vec{M}$$

Applying the simple slab geometry of Figure 6 to

$\nabla x\vec{H} = \frac{4\pi}{10}\vec{J}_c$, yields

$\Delta H_o \simeq \pm\frac{4\pi}{10} J_c\delta$,

and using $H_a - B_{Ave} = \Delta H_o$,

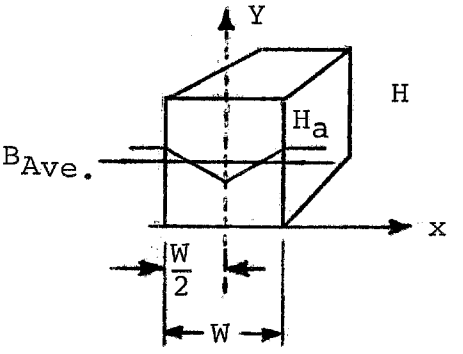

Figure 6.

where δ is the flux penetration distance, one can relate magnetization and critical current by

$$J_c = 10\,\frac{M}{\delta}\,.$$

For the special case where flux penetration from two sides of the slab just meet, $\delta = W/2$, and

$$J_c = 20\,\frac{M}{W}\,.$$

Experimental magnetization curves typically resemble the one shown in Figure 7. The shape will vary depending on the flux pinning characteristics of the superconductor.

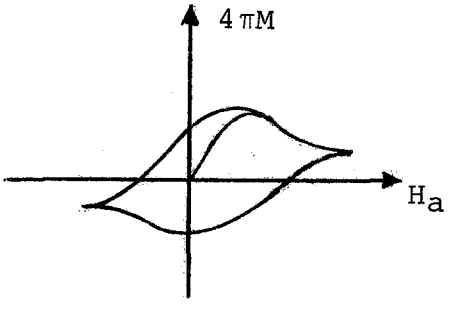

Figure 7.

*Based on an article by H.R.Hart: Proc. 1968 BNL Summer Study, Part II, 571 (1968).

The Bean isothermal, critical state model assumes that the current density J in a superconductor is either = 0 or to $\pm J_c$. Some examples are shown in Figure 8a, 8b and 8c for a high field superconducting slab. The distributions are dependent on the excitation history of the material as is shown in Figure 9. The degree of flux penetration into the slab is temperature dependent as shown in Figure 10 for two uniformly distributed temperatures T_1 and T_2.

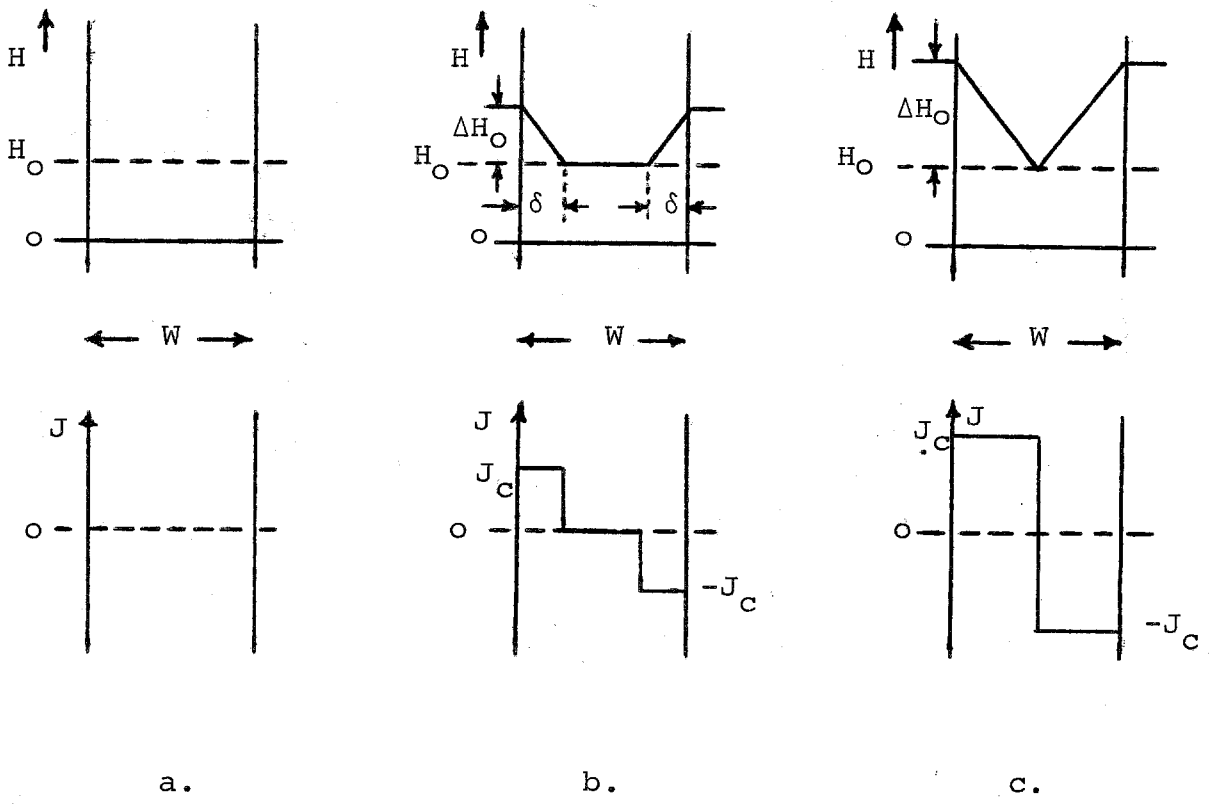

Figure 8. History dependent distribution of field and current density in a high field superconducting slab.*

*Figures 8, 9 and 10 - H.R.Hart, op.cit., pages 590-593.

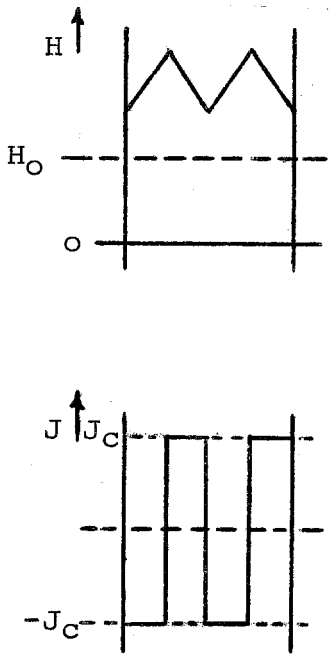

Figure 9. A more complex distribution of the type shown in Figure 7.

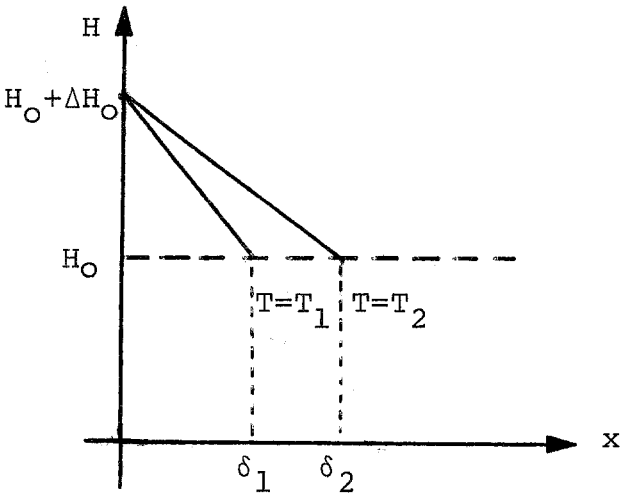

Figure 10. Flux penetration profiles for a semi-infinite superconducting slab at two uniform temperatures.

Adiabatic Stability: When flux moves in a superconductor, corresponding to a change ΔH_o, heat is generated which the material will eventually absorb. One can show that the magnetic heat

$$Q_m \propto (\Delta H_o)^2$$

and the heat absorbed

$$Q_T \propto \int_{T_1}^{T_2} C(T)dT.$$

where C(T) is the heat capacity of the material.

Qualitatively the relations between Q_m and Q_T for stable and unstable operation are shown in Figure 11a and 11b.

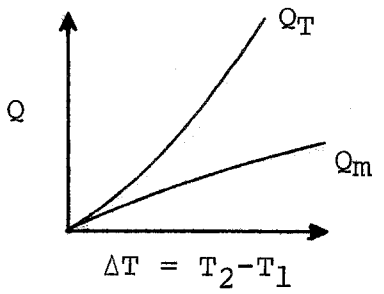

Figure 11a. Stable Operation

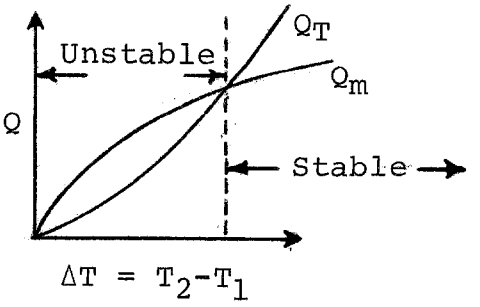

Figure 11b. Unstable Operation

One can derive the temperature changes associated with a particular flux change $\Delta\Phi$. Taking the case, where the temperature rise will cause a quench, $T_2 = T_c$, from

$$\Delta H_o = \{12\pi C(T) \times 10^7 (-\frac{J_c}{\frac{\partial J_c}{\partial T}})\}^{1/2}$$

and assuming that $J_c(T) = J_c(o)(1-\frac{T}{T_c})$,

$$\Delta H_o = \{12\pi C(T) \times 10^7 (T_c - T_1)\}^{1/2}$$

Since Maxwell's equations provide a relationship

$$\Delta H_o \propto J_c d,$$

where d is slab thickness or, in a more interesting geometry, filament diameter. A relationship showing maximum d for stable operation could now be derived. However, enough information is already available to list some conditions required for stability:

a) make C(T), the specific heat, as large as possible,

b) make $\partial J_c/\partial T$ small,

c) make filament diameter small,

d) make J_c small.

The last condition is of course not very attractive in a practical superconductor.

The basic stability situation can be understood in a slightly different way by noting that adiabatic temperature changes should occur if the relationship between thermal diffusivity D_{Th} and magnetic diffusivity D_m satisfies

$$D_m >> D_{Th} \ .$$

The two diffusion equations that apply are thermally

$$D_{Th} \frac{\partial^2 T}{\partial x^2} = \frac{\partial T}{\partial t} \ ,$$

where $$D_{Th} = \frac{k}{C} \ ,$$

and magnetically

$$D_m \frac{\partial^2 B}{\partial x^2} = \frac{\partial T}{\partial t} \qquad , \quad D_m = \frac{\rho_f}{\mu}$$

where ρ_f is the effective flux flow resistivity for the superconductor. Characteristic time constants are then

$$\tau_{Th} = \frac{W^2}{k} \cdot C \quad \text{(Thermal time constant)}$$

and $$\tau_m = \frac{W^2}{\rho_f} \mu. \quad \text{(Field penetration time constant)}$$

where W is a characteristic dimension such as thickness of a slab of superconducting material or diameter of a filament.

THE EFFECTS OF NON-LINEAR HEAT TRANSFER, TERMINAL CHARACTERISTICS AND STABILITY MAPS

Bruce P. Strauss, Energy Doubler, Fermilab

The analysis here concerns the behavior of a short sample of superconductor in a copper matrix which is in good thermal contact in a liquid helium bath and in an externally applied magnetic field. Consider what happens when the current is increased. At low currents, all current flows in the superconductor until it reaches its critical current. If the conductor is well cooled then a further increase results in a "spilling over" of the excess current into the normal matrix.

The net result is the sharing of the total current between the superconductor and the normal substrate. The superconductor must develop some resistance, otherwise it would take on more current. This increase has been characterized by Kim as "flux flow" resistance.[1] Obviously if the temperature is not maintained at or near the bath temperature, the increase in temperature will cause a decrease in critical current. In fact a complete transfer of current can occur. We will now analyze the terminal characteristics of a short sample considering a linear heat transfer coefficient.

Let us define f ($0 \leq f \leq 1$) as the fraction of total current flowing in the substrate. Then the voltage per unit length of conductor is:

$$v = \rho \frac{If}{A} \tag{1}$$

where ρ and A are the resistivity and the cross-section area of the substrate.

Let us now take a heat balance on a unit length of conductor:

$$hP(T-T_b) = vI = \frac{I^2 f}{A} \rho \tag{2}$$

where h is the heat transfer coefficient per unit surface area per unit temperature rise from the conductor to the helium bath at a temperature T_b and for the present is assumed to be constant. The perimeter (here, surface area/unit length) of the conductor exposed to the bath is P.

From this we solve for the temperature rise at the wire

$$T-T_b = \frac{\rho I^2 f}{hPA} \tag{3}$$

Under conditions of current sharing, T and B external determine the critical current in the superconductor. We define $I_{ch}(T_b)$ as the critical current at the bath temperature and given applied magnetic field. This is the short sample value of the superconductor. The relationship to current in the superconductor at a temperature T can be given as:

$$\frac{I_s}{I_{ch}} = \left[1 - \frac{T-T_b}{T_{ch}-T_b} \right] \tag{4}$$

where T_{ch} is the zero current critical temperature at the applied field.

Let us now define a stability parameter.

$$\alpha \equiv \frac{\rho I_{ch}^2}{hPA(T_{ch}-T_b)}$$

This is just the ratio of the heat generated per unit length to the heat that can be taken away by the bath. Using α and Equations (1) and (2) we can obtain the following:

$$= \frac{\tau-1}{\tau(1-\alpha\tau)} \tag{5}$$

$$\frac{vA}{\rho I_{ch}} = \frac{\tau-1}{1-\alpha\tau} \tag{6}$$

$$\theta = \frac{\alpha\tau(\tau-1)}{1-\alpha\tau} \tag{7}$$

where

$$\tau = I/I_{ch}$$

$$\theta = \frac{T-T_b}{T_{ch}-T_b}$$

Figure 1 shows the terminal characteristics predicted by Equation (6). For $\alpha<1$ no voltage appears until $I = I_{ch}$ and then the voltage increases gradually with current. For $\alpha>1$ the operation is more complicated.

For $$0<\tau\leq\frac{1}{\sqrt{\alpha}}$$

single valued operation occurs in the superconductor.

For $$\frac{1}{\sqrt{\alpha}} \leq\tau\leq 1$$

single valued operation occurs with all the current in the substrate since operation in the negative resistance portion of this curve is unstable for constant current type of operation.

For $\tau>1$

single valued operation occurs with all the current in the substrate.

NON LINEAR HEAT TRANSFER

For purposes of discussion we approximate the heat transfer characteristic to helium as shown in Figure 2. This gives us a constant heat transfer coefficient region and a constant heat flux region.

In the constant heat transfer coefficient region the previously obtained relationships apply. In the constant heat flux or film boiling region:

$$q = q_{max} = h(T_m-T_b)$$

This represents a constant power dissipation and therefore:

$$hP(T_m-T_b) = \rho\frac{I^2 f}{A}$$

Putting this into the same form as Equations (6), (7) and (8) we find:

$$f = \frac{\theta m}{\alpha\tau^2} \tag{8}$$

$$\frac{vA}{\rho I_{ch}} = f\tau = \frac{\theta m}{\alpha\tau} \tag{9}$$

$$\theta = \frac{\theta m+\alpha\tau(1-\tau)}{\alpha\tau} \tag{10}$$

where

$$\theta m = \frac{T_m-T_b}{T_{ch}-Tb}$$

we can again obtain terminal characteristics for a short sample. For $\alpha<1$ three points will characterize the curves.

a) The critical current where

$$I/I_{ch} = 1.0$$

b) The transition from nucleate to film boiling where current is shared. This is solved by equating Equations (9) and (6) and solving for

$$\frac{I}{I_{ch}} = \frac{1-\theta m}{2} + \left(\left(\frac{1-\theta m}{2}\right)^2 + \frac{\theta m}{\alpha}\right)^{\frac{1}{2}}$$

c) The recovery from film to normal boiling with all the current in the substrate. This is the f = 1 point in Equation (8) so

$$\frac{I}{I_{ch}} = \left(\frac{\theta m}{\alpha}\right)^{\frac{1}{2}}$$

BEHAVIOR MAP

From the above a behavior map can be drawn as shown in Figure 3. This has the following regions and curves:

a) The short sample curve.

b) The recovery curve - defined by the condition for maximum nucleate boiling heat flux when all the current is in the substrate.

c) The take off curve - defined by the condition for maximum nucleate boiling heat flux under conditions of current sharing ($f \leq 1$).

d) Stable zero resistance region - below the recovery and short sample curve.

e) Stable resistance region - above the short sample curve and below the recovery curve.

f) Metastable region - between the takeoff and recovery curves.

g) Unstable region - above the takeoff curve.

References

1. Y.B.Kim, C.F.Hempstead and A.Strnad, Phys. Rev. Letters 9, 306 (1962).

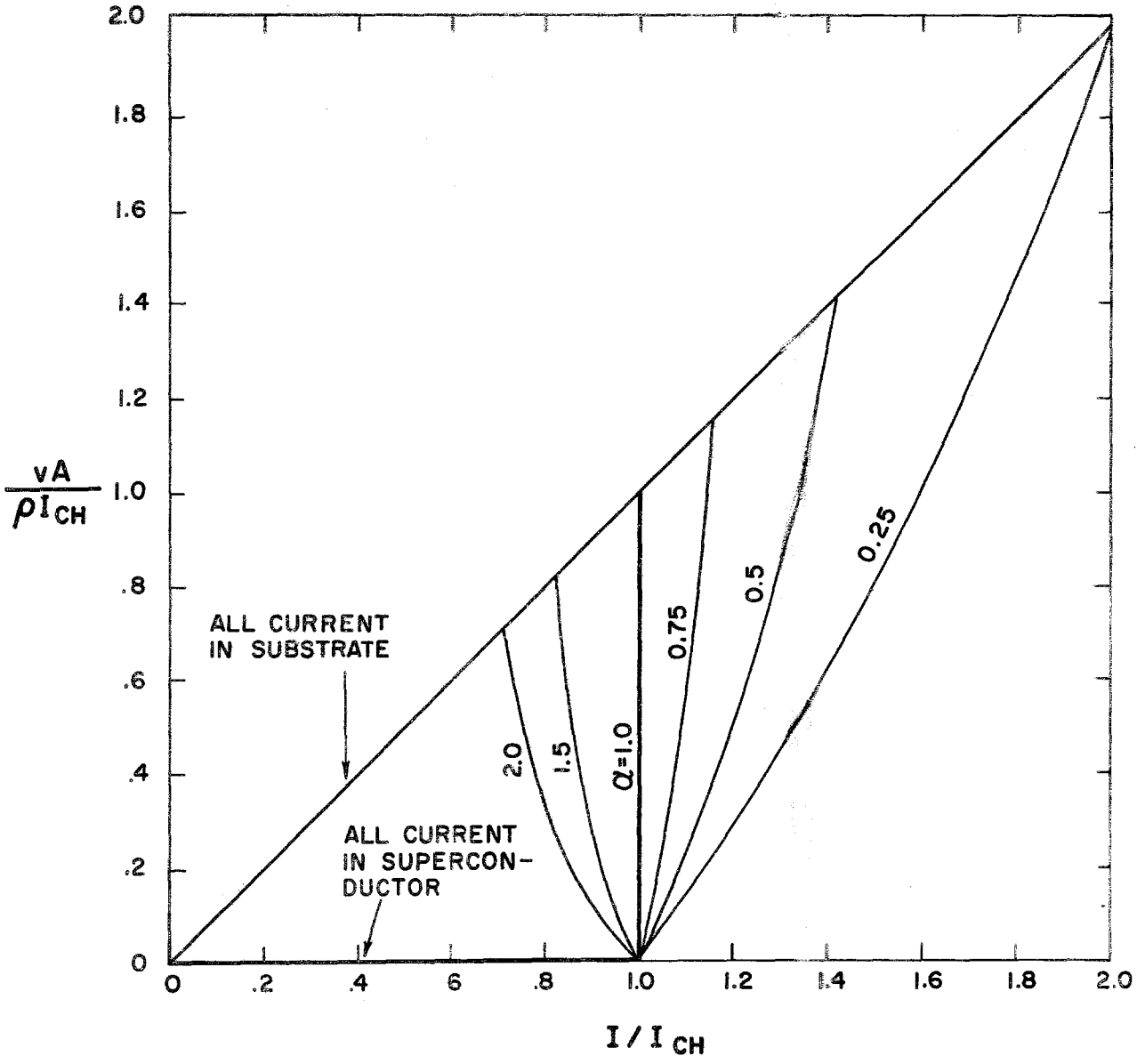

Fig. 1 Voltage - current characteristics for a stabilized superconductor - substrate combination

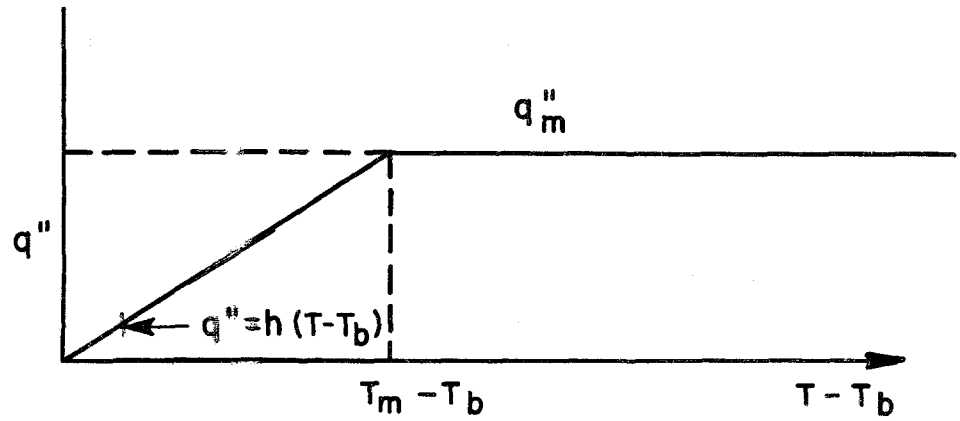

Fig. 2. The idealized heat transfer characteristic - first approximation.

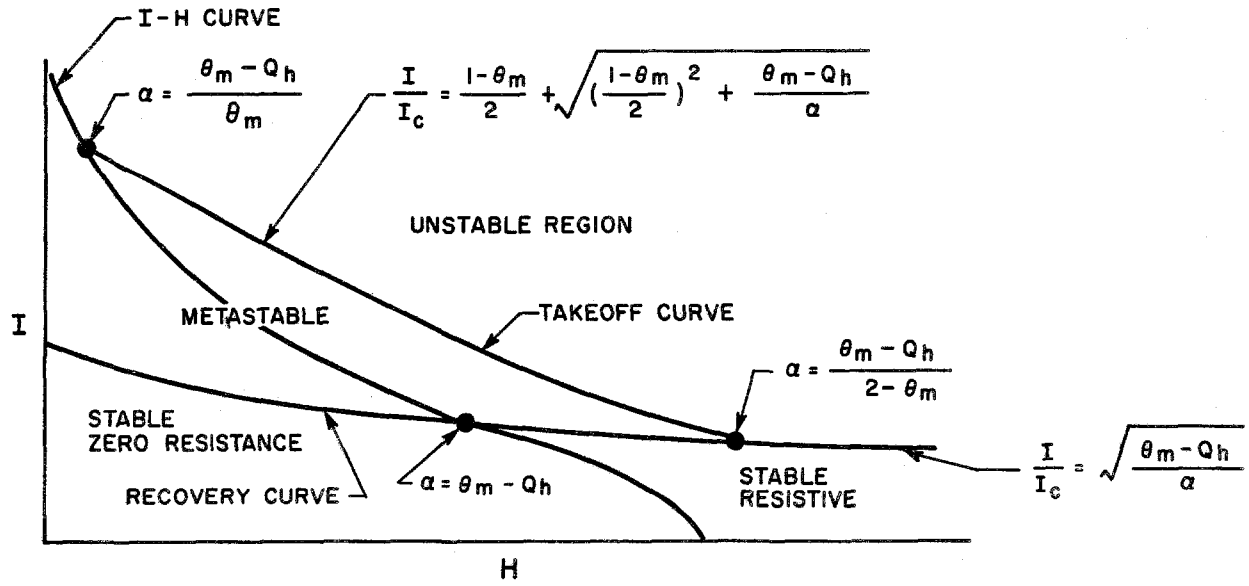

Fig. 3. Map indicating modes of behavior as predicted by a zero-dimensional analysis incorporating a nonlinear heat transfer characteristic.

DYNAMIC STABILITY

Darrell Drickey, Energy Doubler

Fermilab

In adiabatic stability the thermal properties of the superconductor itself are sufficient to prevent an adiabatic local field change from raising material temperatures enough to drive the superconductor normal. Dynamic stability attacks the other side of this problem; that is, the physical properties of the copper-superconductor matrix are examined and one attempts to interdict the heat generating mechanism - the rapidly changing local field. The rate of heat generation is thereby sufficiently limited so that the natural heat dissipation properties of the conductor will prevent any local temperature from becoming equal to or greater than critical temperature, T_c.

In Type II superconductors an increase in temperature results in a reduction of J_c ($\partial J_c/\partial T < 0$). A change in J_c will cause some reconfiguration of flux ($\Delta\Phi$) which implies further heat generation and a resulting temperature rise.* Thus a cycle is created,

$$\Delta T_1 \rightarrow \Delta J_c \rightarrow \Delta\Phi \rightarrow \Delta Q \rightarrow \Delta T_2$$

This process can be regenerative,

$$\frac{\Delta T_2}{\Delta T_1} \gtrsim 1,$$

which is the unstable mode, or it can be damped,

$$\frac{\Delta T_2}{\Delta T_1} < 1,$$

---

*See H. Brechna, Superconducting Magnet Systems, page 303 ff.

which is the necessary condition for stability. Basically, the copper's electrical properties must be such that flux motion is slowed sufficiently to allow adequate heat transfer from the superconductor to the helium bath.

The cycle outlined above provides a program for computation of the ratio $\Delta T_2/\Delta T_1$. As an example consider an infinitely long cylindrical superconductor surrounded by a concentric layer of normal metal matrix. Solution of the diffusion equation for the finite local temperature rise, $\Delta T = f(r, \phi, t)$, in this geometry and application of the boundary conditions: at time $t = 0$, $\Delta T = \Delta T_1$ at $r<d/2$ and at $r\geq d/2$, $\Delta T = 0$,* will lead to

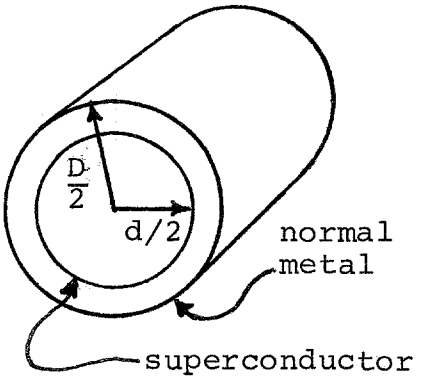

$$\frac{\Delta T_2}{\Delta T_1} = \frac{\pi^2}{6} \frac{d^2}{23\ k_s} \frac{d/D}{1-d/D} \rho_{Cu} J_c^2 \left(-\frac{1}{J_c} \frac{\partial J_c}{\partial T}\right).$$

Using the condition that $\Delta T_2/\Delta T_1 < 1$ then requires

$$d^2 \lesssim \frac{138}{\pi^2} \frac{k_s}{\rho_{Cu}} \frac{1-d/D}{d/D} \frac{1}{J_c^2} \left(\frac{J_c}{\partial J_c/\partial T}\right)$$

where k_s is the thermal conductivity of the superconductor and ρ_{Cu} the resistivity of the copper matrix. One can also compute the thickness of the copper matrix required for a quench. Expressed in terms of the magnetic diffusivity of the copper matrix

$$D_m = \frac{\rho_{Cu}}{\mu_o}$$

*Brechna, op. cit., page 314, assumes that heat transfer to the bath and thermal conductivity in the normal metal are both infinite.

and the thermal diffusivity

$$D_{Th} = \frac{k_s}{C_s}$$

again k_s is thermal conductivity and C_s the heat capacity of the superconductor. Then the condition $\Delta T_2/\Delta T_1 < 1$ requires

$$(D-d) \gtrsim \frac{\pi^2}{138} d^3 \frac{\pi}{C_s} \frac{D_m}{D_{Th}} J_c^2 \left(-\frac{1}{J_c}\frac{\partial J_c}{\partial T}\right).$$

From

$$\nabla \times \vec{B} = 4\pi \vec{J}_c$$

and assuming a wire whose length $l >> d$, application of Stoke's theorem shows

$$B \propto J_c\, d.$$

where B is the full penetration field for the superconducting filament, and J_c is the critical current density. This demonstrates that any condition on d is also a condition on the field, B, at the surface of the superconductor.

Thus one can conclude that to have dynamic stability one must control a) the rate of motion of flux in the composite and b) the rate at which conductor surface fields can change as a result of either deliberate changes in current or perturbations in the external field.

One of the purposes of this Workshop is to try and understand some of the phenomena seen in Energy Doubler prototype magnets. Training has generally been associated with mechanical motion of individual wires or of the structure as a whole, a so-called pressure bottle model. To relate wire instabilities arising from phenomena explained by the models of dynamic or adiabatic stability presented in these talks requires that certain

phenomenology characteristic of magnets exhibiting training be explained. The two most important characteristics are the progressive increase of quench currents on successive cycles and the phenomena of memory wherein the higher operating current limits achieved on successive quenches are remembered, even after a warm-up to room temperature in some cases. Two variations of these phenomena occur. Sometimes a partial relapse occurs with a warm-up to room temperature, and in fact some magnets have been reported to have no memory at all - although none of the Doubler magnets have failed to exhibit considerable memory. Occasionally a relapse will occur during a run where no warm-up has occurred.

None of the theories presented in this Workshop would seem to contradict the statement that remembered training represents a permanent mechanical reconfiguration of the magnet coils. The question of the triggering mechanism which initiates a quench is not so clear. One must now ask which is cause and which is effect. Does the sudden release of energy start because of mechanical motion that releases heat in the process of assuming a lower stored energy configuration, or is the quench triggered by some property of the wire and the mechanical rearrangement of the structure a result of the high differential stressing caused by rapidly collapsing fields and sudden thermal expansion of materials?

Tests have been made to try and determine if gross structural motion or individual wire motion was the principle cause of quenching. Voltage taps placed across each half shell show that almost all quenches originate in the inner shell pair. At-

tempts to alter training patterns by powering first the inner and then the outer shell pair separately confirmed inner shell training and showed that outer shells could be trained to $\gtrsim$3000A.

Eventually we were led to the I_1 versus I_2 tests of 2 1/2 foot magnet #5 where the current I_2 in the outer shell of the magnet was set at a fixed value, and the inner shell current I_1 was ramped up until a quench occurred. The results are presented in Figure 1. Attempts to fit the data of Figure 1 by a constant wire-force model such as $B_1 I_1 = (K_1 I_1 + K_2 I_2) I_1 =$ constant, where K_1 and K_2 are appropriate excitation constants for fields due to inner shell and outer shell respectively, or by treating the structure as a pressure vessel in which the Maxwell stress tensor implies $(K_1 I_1 + K_2 I_2)^2 =$ constant have all been unsuccessful. The only successful fit thus far has been supplied by Tom Collins of Fermilab who has found that the lower part of the I_1 vs. I_2 plot in Figure 1 fits a constant worst field in the inner shell of 27.8 kG and a constant 30.8 kG worst field over the upper part of the graph.

The fit of the I_1 vs. I_2 data does not seem to relate to adiabatic or dynamic stability, which are inherently low field criteria, nor does it seem consistent with mechanical motion of wires or structures. On the basis of the Collins emperical fit the data does seem to perhaps be relevant to a high field stability criteria. While this topic is not covered specifically in this Workshop, work has been done in this area at other laboratories and it will certainly be pursued further at Fermilab.

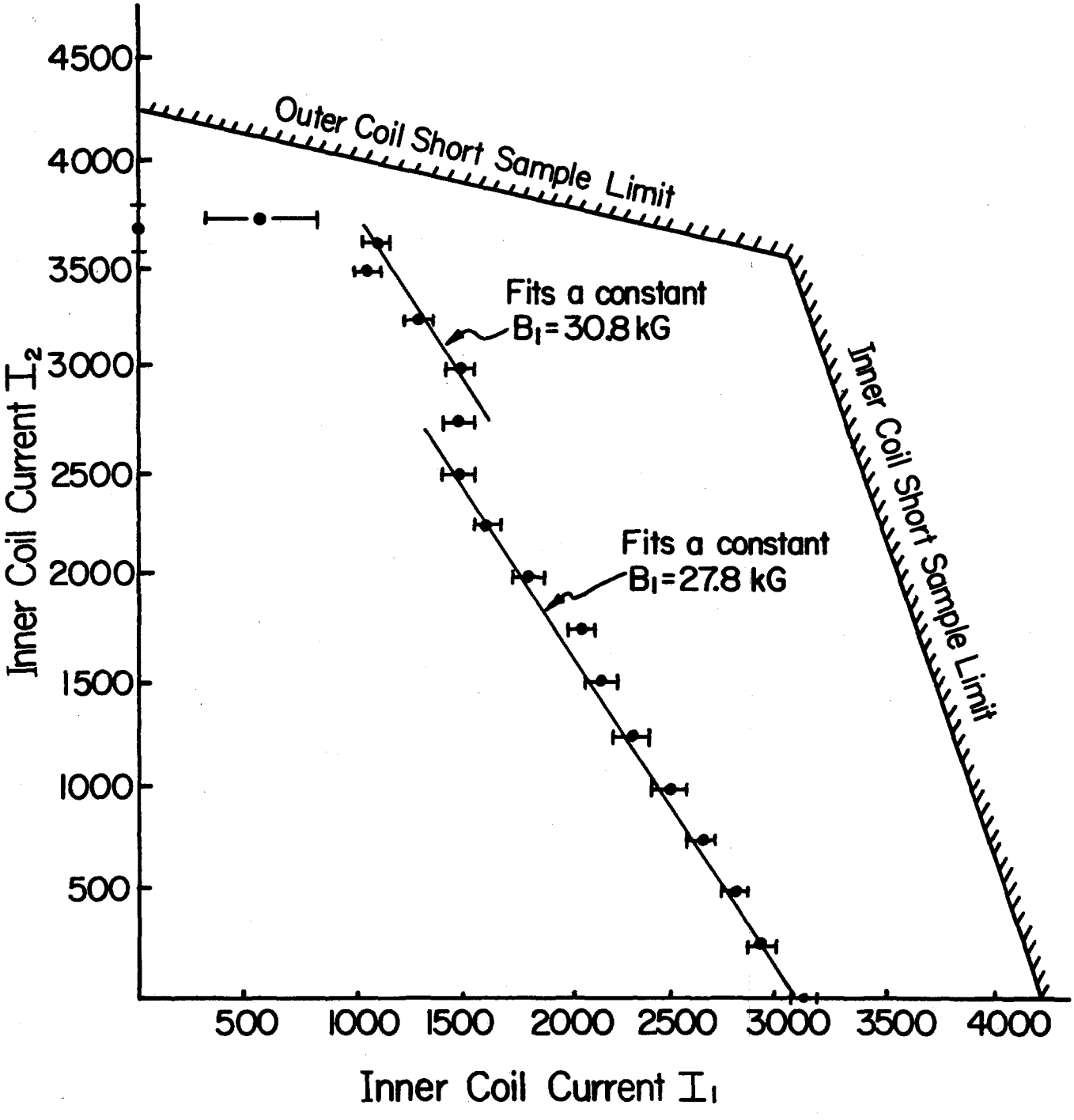

Figure 1. Outer coil current versus inner coil current for 2 1/2 ft #5. B_1 is the highest field value at any conductor in the inner shell. All quenches started in inner coils. Five quenches were taken per point and averaged.

ADIABATIC STABILITY

P.A.Sanger, Energy Doubler, Fermilab

When the local magnetic field in a Type II superconductor undergoes a sudden change or "flux jump", heat is generated. If this change occurs so quickly that the heat generated cannot diffuse away from the region of local field change, then an adiabatic temperature rise occurs which, if sufficiently large, can create a local normal zone.

To place the discussion in a more quantitative framework; under some conditions magnetic diffusivity D_m may be much greater than thermal diffusivity D_{Th}. Then isothermal conditions are not maintained when a local field change occurs, and, in the limit $D_m >> D_{Th}$, the resulting local temperature change ΔT_1 can be considered adiabatic. Since critical current in a superconductor generally decreases with increasing temperature, further flux is allowed to penetrate, generating more heat, and an additional temperature rise ΔT_2 occurs. If $\Delta T_2 > \Delta T_1$ a thermal runaway is initiated, resulting in a normal zone and quench of the magnet.

To determine conditions for adiabatic stability let us calculate 1) Q_m = heat generated in a flux jump, 2) Q_T = heat absorbed by the material (due to its heat capacity) and ask what conditions must be imposed on conductor characteristics to ensure that the stability condition

$$\frac{dQ_m}{d_T} < \frac{dQ_T}{d_T} \qquad (1)$$

be met.

If T is the temperature in the superconductor, T_c the critical temperature and T_b the temperature of the helium bath one can examine the values of Q_m and Q_{Th} as a function of $T_c - T$ and see what relative values will provide adiabatic stability. In Figure 1, dQ_T/dT is clearly everywhere greater than dQ_m/dT and stability occurs for all values of $T_c - T$.

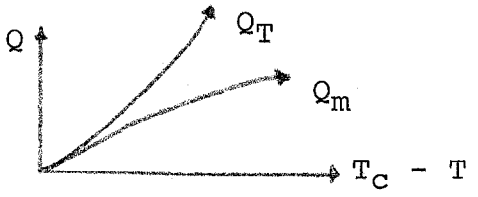

Figure 1.

Stable everywhere.

In Figure 2 the region where $Q_m \geq Q_T$ corresponds to a region in which $\frac{dQ_m}{d_T} < \frac{dQ_T}{d_T}$ and one has unstable operation.

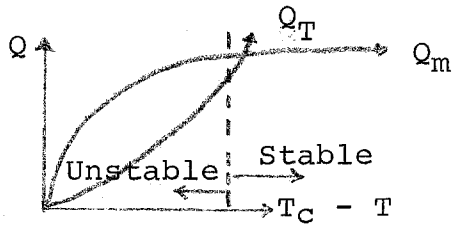

Figure 2.

When $Q_T > Q_m$, the condition for stability is reasserted due to the functional characteristics of Q_m and Q_T.

Let us examine these functional characteristics. One can show that the energy dissipated as heat in a flux jump is given by the total energy into the slab less the magnetic energy,

$$Q_m = \int_{t_1}^{t_2} 10 \left(\frac{\vec{E}x\vec{H}}{4\pi}\right) dt - \frac{10^{-7}}{8\pi}\int_0^{\infty} [H_2^2(x) - H_1^2(x)]dx \quad . \quad (2)$$

The integration is carried over the volume element dx in slab geometry. Generally

$$Q_T = \int_{T_1}^{T_2} C(T)dT \quad (3)$$

when C(T) is the heat capacity of the material.

Assuming

$$C(T) = C(T_b)\ (T/T_b)^3 (erg/cm^3 °K)$$

and $$J_c(T) = J_c(o)\left[1-\left(\frac{T}{T_c}\right)\right]$$

one can compute the incremental field change ΔH_o required to produce unstable performance by simply equating dQ_m/dT and dQ_T/dT. Thus

$$\frac{dQ_m}{dT} \leq C(T) \quad (4)$$

which becomes[1,2]

$$\Delta H_o = \left[12\pi C(T_b)\left(\frac{-J_c}{\partial J_c/\partial T}\right)\right]^{\frac{1}{2}} (general) \quad (5)$$

$$= \left[12\pi C(T_b)(T_c - T_b)\right]^{\frac{1}{2}} \left(for\ \frac{\partial J_c}{\partial T} = constant\right) \quad (6)$$

where $[C(T_b)] = erg/cm^3 °K$

$[T] = °K$

$[\Delta H_o] = gauss$

Two representative cases have been computed with results shown below. In both cases, T_c and C_1 for NbTi are taken as 8.9°K and 10.1×10^3 erg/cm^3°K at 4.2°K respectively.

Case 1. $J_c = J_o(1-\frac{T}{T_c})$ (Eq.6)

T(°K)	ΔH_o(kgauss)
3	.9
4.2	1.3
5	1.6

Case 2. Experimental data from Reference 3. (Eq.5)

$J_c \frac{\partial J_c}{dT}$(°K)	H(kG)	T(°K)	ΔH_o(kG)	d(mils)
8.08	30	3	1.06	6.6
3.02	30	4.2	1.07	8.3
18.9	0	4.2	2.68	3.3

The calculated ΔH_o can be converted into a meaningful design parameter by applying the Bean model to a small filament of superconductor. The maximum flux jump occurs when the field penetrates to the center of the filament. In order to establish stability, this maximum flux jump must be less than the critical flux jump from Eq. 5.

$$\nabla x \vec{H} = \frac{4\pi}{10} \vec{J}_c$$

$$\Delta H = \frac{\pi J_c d}{10}$$

then

$$\Delta H_o = \frac{\pi J_c d}{10} \leq [12\pi C(T_b)(\frac{-J_c}{\partial J_c/dT})]^{\frac{1}{2}}$$

$$d \leq \frac{10}{\pi J_c} [12\pi C(T_b)(\frac{-J_c}{\partial J_c/dT})]^{\frac{1}{2}}$$

Typical required filament diameters were calculated for Case 2. From this certain general conclusions may be reached. To obtain adiabatic stability

1. increase C(T)
2. reduce $\frac{\partial J_c}{\partial T}$, ideally $\frac{\partial J_c}{\partial T} > 0$
3. make $d_{filament} < d_{critical}$

References:

1. H.Hart, 1968 Superconducting Summer Study, Brookhaven p. 571.

2. H.Brechna, Superconducting Magnet Systems, 305 ff.

3. K.Wohlleben, J.Low Temp. Phy., 13, 269 (1973).

MECHANICAL INSTABILITIES

J. R. Heim

Inelastic behavior of the matrix metal used to stabilize superconductors should be treated as a mechanical loss which generates heat. These mechanical losses can be identified by material testing and eliminated with good design, careful construction and post wind preloading.

We begin our study by considering the metallic partners making up the composite. Copper is a good superconductor stabilizing metal in the softened condition but a poor structural material. Niobium titanium, on the other hand, is radically different. NbTi is a tough metal with a very high elastic strain capability. Also, the expansion coefficients of the two metals differ by more than a factor of 2. In line with the above considerations, we can expect that the manufacturing processes develop significant residual stresses and we should estimate the magnitude of same.

Manufacturing Process Effects

The following assumptions were then made about the manufacturing process.

(1) At final draw both metals exit the drawing die stressed to their ultimate strength.

(2) The wire is wound tightly on a steel spool for heat treatment.

(3) The copper final heat treatment is to the full anneal condition.

Using these three assumptions and a compression stress-strain curve for annealed copper, we can calculate the residual stresses in both wire components. Residual stresses are plotted below as a function of the copper to superconductor ratio for both room temperature and liquid helium temperature.

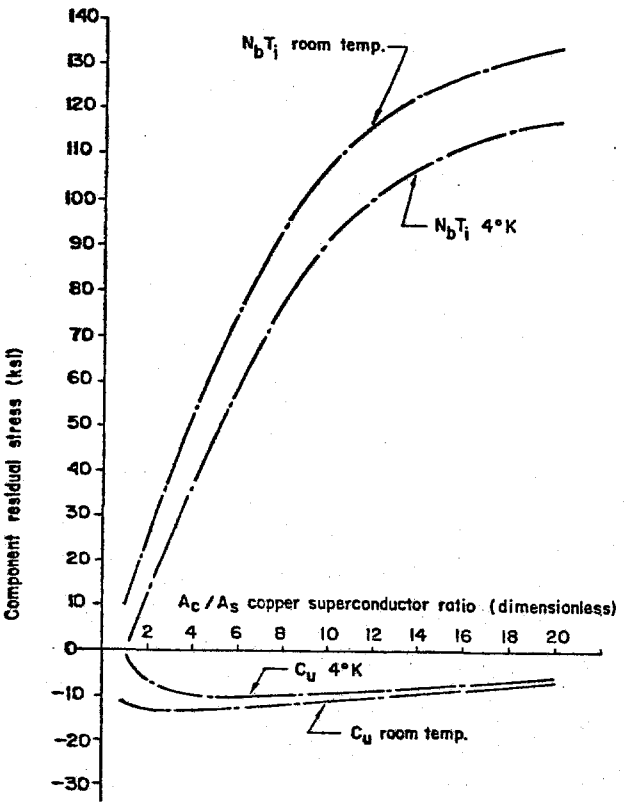

Manufacturing Process Residual Stresses

Twisting

One of the processes used to manufacture superconducting wire is twisting. To evaluate the effects of twisting, an expression was developed which describes the NbTi stress distribution across the wire cross section with respect to axial strain.

$$\sigma_k = E_s \left[\frac{(\varepsilon+1)^3}{(\varepsilon+1)\quad(n^2\pi^2d_k^2+1)}\right]^{\frac{1}{2}} - E_s \left[\frac{(\varepsilon+1)^3}{n^2\pi^2d_k^2+(\varepsilon+1)^3}\right]^{\frac{1}{2}}$$

where,

σ_k = circular element average stress

E_s = superconductor modulus of Elasticity

d_k = circular element mean diameter

ε = wire strain (axial)

n = number of twists per inch

This equation can then be solved using numerical methods. For our test specimen (to be shown later) twisting represents a 6% effect which was accounted for analytically by using an effective modulus of elasticity which is reduced by 6%.

Bending Effects

Next we study the effects of spooling (bending) on the stress distribution across the wire cross section. We assume a 13,000 psi residual compressive stress in the copper component (our specimen) and we adopt a simplified stress-strain diagram made up of three straight lines representing (1) inelastic compression, (2) elastic range, (3) inelastic tension. We determine graphically the strain differential corresponding to some extreme fiber being stressed to its tensile elastic limit and solve for the corresponding radius of curvature. We interpret the results as follows: If the wire is bent to a radius less than 333 wire diameters, it will exhibit inelastic behavior only when tensile load is applied. Since most wire is wound onto spools with a radius much smaller than 333 wire diameters, testing should show inelastic behavior at the onset of loading.

The Bauschinger Effect

Another stress-strain interaction between wire components which may have an important effect on superconducting coil performance is the Bauschinger Effect. If a material is loaded in tension beyond the elastic limit, the elastic limit in tension is increased but the elastic limit in compression will be decreased. Similarly for compressive loading beyond the elastic limit the elastic limit in tension will be decreased. This effect will be used later to explain why poorly designed superconducting coils train to an upper limit which is lower than the design goals.

Tests and Results

A superconducting wire specimen was chosen for tensile testing. Specimen wire data is shown below:

Material	- NbTi with a Cu matrix
Size	- .040" diameter round wire
Copper to superconductor ratio	- 4/1
Number of filaments	- 84
Twist pitch	- 2 per inch

A test specimen approximately 100 inches long was then set up as shown below.

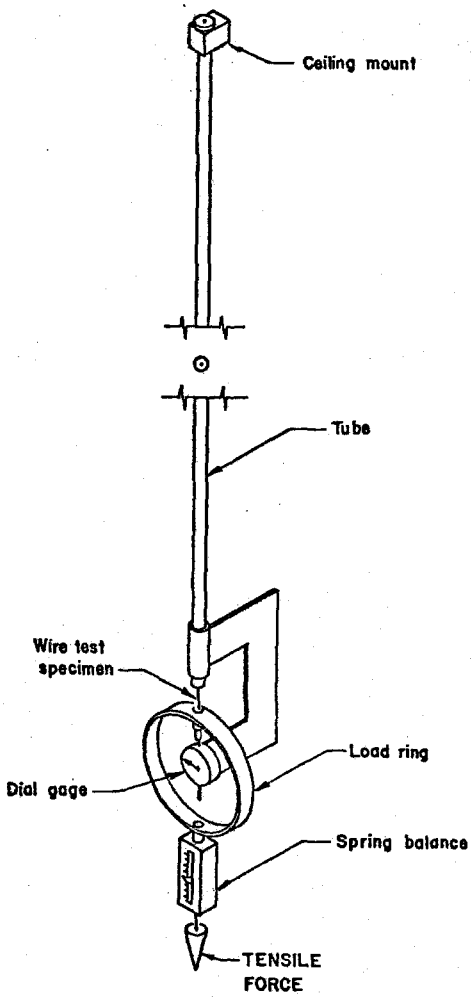

Tensile Test Set Up

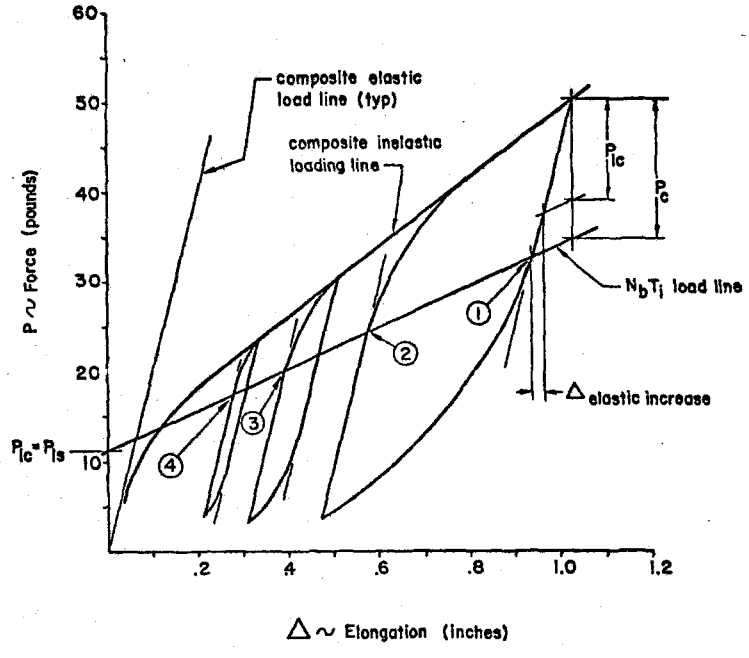

Tensile Test Results

The load-elongation data shown above was obtained by loading the wire specimen in tension and unloading and reloading the wire to form the hysteresis loops shown.

The first step in evaluating the test data was to determine what part of the applied load was carried by the NbTi. Since the NbTi behaves elastically its load line will be linear with a slope of,

$$\text{Slope} = \frac{\cdot 94\ As\ Es}{\ell}$$

where,

As = NbTi cross sectional area
Es = NbTi modulus of elasticity
ℓ = specimen length
•94 = twist correction factor

The location of the NbTi load line on the test data plot was then determined in the following manner. For the large hysteresis loop shown at the right, point 1 is the transition from elastic to inelastic behavior of the composite wire for the unloading condition. Since the NbTi behaves elastically, point 1 must be the elastic limit of the copper in compression and the force transmitted through the NbTi component must be greater than or equal to the applied load, i.e., the NbTi load line must pass through point 1 or above it. Similarly, point 2 corresponds to the elastic limit of the copper in tension and the NbTi load line must pass through point 2 or below it. The NbTi load line was then added to the test data plot and the load line passed through both points 1 and 2. The NbTi load line also passed through points 3 and 4 which are the elastic limits of the copper in tension for the smaller hysteresis loops. It then follows that the intersection of the NbTi load line and the vertical coordinate is the tensile loading in the NbTi for zero applied load and this value must be equal to the compressive load in the copper prior to the specimen testing. For our specimen the preloading in the copper component is 11 pounds which corresponds to a compression prestress of approximately 11,000 psi. The agreement between this measured value (11,000 psi) and the calculated value (13,000 psi from residual stress plot) is considered good for the assumptions made with respect to the manufacturing process.

The three hysteresis loops show the Bauschinger Effect very well. Precompression of the copper due to the manufacturing process had decreased the copper tension elastic limit to zero and the copper component of our superconducting

wire has an initial elastic strain capability of

$$\varepsilon_{elastic} = \frac{\sigma_{ic}}{E_c} = \frac{P_{ic}}{A_c E_c}$$

where subscript ic refers to initial copper and P_{ic} is the negative of the vertical intercept shown by the test data.

Tensile loading and unloading of the specimen strain hardens the copper very little and the load reversal experienced by the copper shifts the tension and compression elastic limits of the copper such that Bauschinger loops are developed. The two smaller hysteresis loops show the copper compressive elastic limit to be decreasing (shifting toward the NbTi load line) while the larger loop shows the copper elastic limit to be reduced to its limiting value of zero.

Coil Thermal Response

To evaluate the heating potential of the above mechanical losses the thermal response is presented as a temperature rise independent of all other heating and cooling effects. Thermal calculations were simplified by assuming that the specific heat of the NbTi is the same as copper for our temperature range. The enthalpy rise was then calculated as

$$\Delta h = \frac{\text{hysteresis loop area}}{\ell A \rho J}$$

where

ℓ = specimen length
A = specimen cross sectional area
ρ = density
J = Joules constant

and the corresponding conductor temperature was read on a temperature-enthalpy diagram for copper.

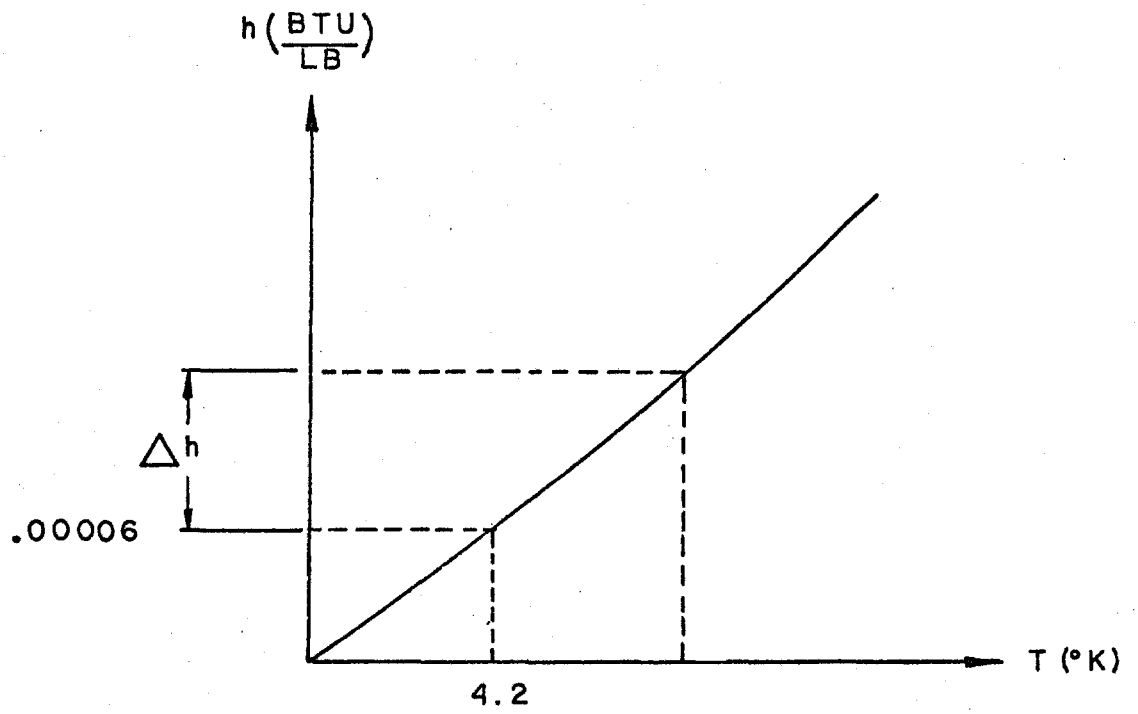

Copper Temperature - Enthalpy Plot

The heating potential (Δh) and potential conductor temperature for the three hysteresis loops are shown below.

Test Data	Heating Potential $(\frac{BTU}{lb.})$	Potential Coil Temp. (°K)
Small loop	.00077	9.4°K
Intermediate loop	.0032	14°K
Large loop	.0231	23°K

Coil Training

The next interpretation of our test results is a description of coil training which is due to inelastic behavior of the copper. The following description is considered qualitative only, i.e., a quantitative analysis must account for all heating and cooling peculiar to a specific coil design and operating system.

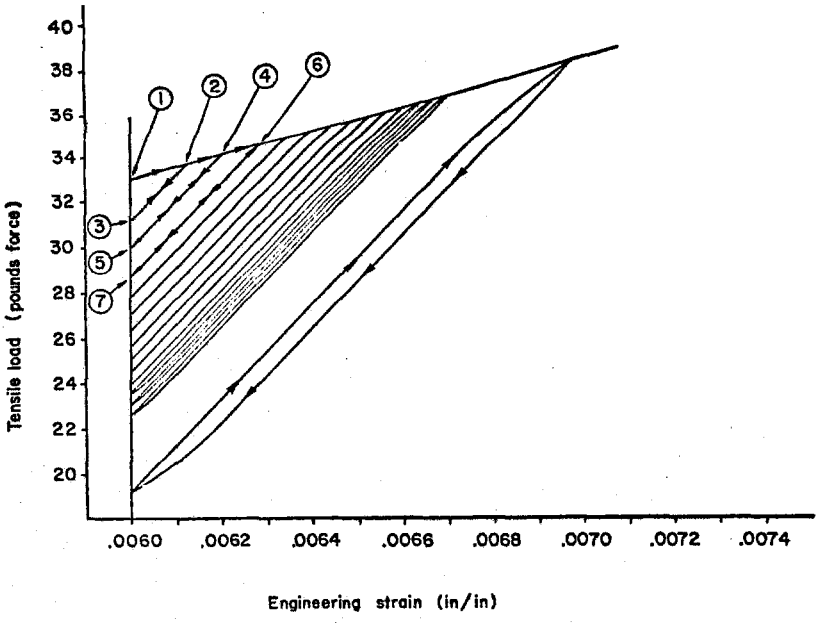

Graphical Description of Training

Point 1 in the above figure represents the initial condition of our wire specimen prior to charging the coil for the first time. When the coil is energized for the first time, the coil experiences plastic deformation at the onset of loading and proceeds to point 2 where the coil quenches. The wire then unloads along line 2-3 (elastic behavior) to point 3. When the coil is energized a second time the wire reloads along the line 3-2 and then proceeds to point 4 where the coil quenches again. In this manner the coil continues to train to higher levels but the training gain becomes progressively smaller. The strain excursion eventually exceeds the initial elastic strain capability of the copper calculated previously $(\frac{\sigma_{ic}}{E_c})$ and Bauschinger loops begin to develop. Finally, after many quenches the coil trains to its design value. The hysteresis loop shown represents the final Bauschinger loop for a coil designed to operate with a strain excursion of approximately .001 inches per inch. For this example the coil has trained satisfactorily to full field, however, the coil performance may not be satisfactory if the charge time is limited. Approximately half of the heat generated by the hysteresis loop is generated during the final 15% of the strain excursion at the end of the charge transient and this rate of heat generation may limit the charge time to

longer periods than the design value. Finally, for poorly designed coils severe Bauschinger loops may develop at currents and fields well below the design goals such that the coil will never reach its design values.

How to Eliminate Mechanical Losses

(1) Don't use soft copper. Cold work the copper a modest amount to increase its elastic strain capability,

(2) Eliminate spooling, handling and coil winding effects with the PWP process.

The PWP (post wind preload) process can be used to change the stress distribution in the copper component of superconducting wire so that the copper will behave elastically during coil operation. After the coil has been completely wound a system of forces is applied to the coil and the strain experienced by the copper changes the stress distribution in the copper. In simple terms we might describe the process effect as a history eraser. The undesirable effects of spooling, handling, etc., are eliminated by prestressing the copper to a level greater than the operational stress. One method of performing the PWP process is shown below.

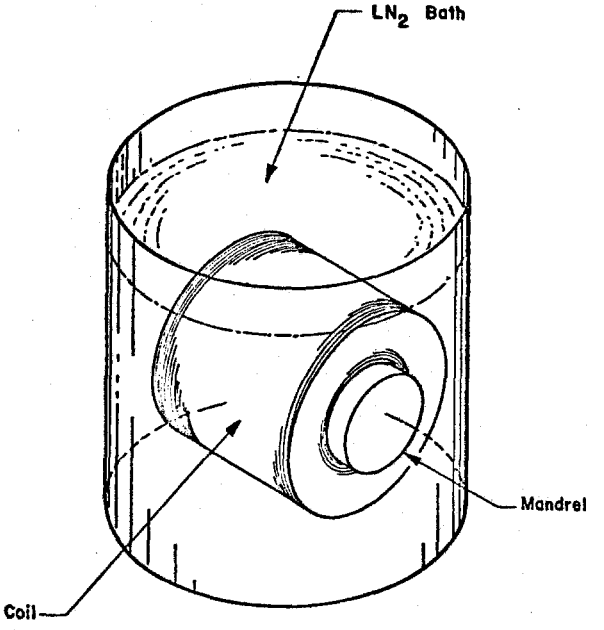

The PWP Process

The coil (solenoid shown) is wound on a mandrel made from a material which has a very low coefficient of expansion (invar or equivalent). After the coil is completely wound and cured (potted construction assumed) the coil with mandrel is cooled to 77°K with liquid nitrogen. Due to the contraction differential between copper and mandrel, the copper component of the coil turns adjacent to the bore will experience hoop strains approaching 0.3%. The coil is then warmed to room temperature and the mandrel is removed which completes the process.